bioengineering

MDPI

Article

Impact of Phage Cocktail Application on the Microbiota of Saline Produced Water During Ammonia Removal

Lutecia Rigueira Medina [1], Maíra Paula de Sousa [2], Alex Gazolla de Castro [1], José Junior Ferreira Soares [1], Rodrigo Suhett de Souza [2], Sérgio Oliveira de Paula [3] and Cynthia Canedo da Silva [1,*]

[1] Department of Microbiology, Federal University of Viçosa, Viçosa 36570-900, MG, Brazil; lutecia.medina@ufv.br (L.R.M.); alex.gazolla@ufv.br (A.G.d.C.); jose.j.soares@ufv.br (J.J.F.S.)
[2] Leopoldo Américo Miguez de Mello Research and Development Center, Petrobras, Rio de Janeiro 21941-915, RJ, Brazil; mpsousa@petrobras.com.br (M.P.d.S.); rsuhett@petrobras.com.br (R.S.d.S.)
[3] Department of General Biology, Federal University of Viçosa, Viçosa 36570-900, MG, Brazil; depaula@ufv.br
* Correspondence: ccanedo@ufv.br

Abstract

Bacteriophages offer a targeted approach to industrial biocontrol, with the potential to control undesirable bacteria while limiting direct effects on nonsusceptible microorganisms. However, their compatibility with microbial functions essential to saline produced-water treatment remains poorly understood. This study evaluated produced-water treatment microcosms after a single application of a four-phage cocktail at 10^7 PFU mL^{-1}. Sludge that acclimated to 55 or 125 g L^{-1} NaCl was monitored for ammonia removal, infective phage persistence, cell membrane integrity, and prokaryotic community composition. Control microcosms maintained ammonia removal above 94%, whereas treated systems showed a transient reduction after cocktail application. Ammonia removal recovered to above 90% by day 16 at 55 g L^{-1} NaCl and by day 55 at 125 g L^{-1} NaCl, indicating a more persistent response at higher salinity. Infective phage titers declined by day 6 and were undetectable from day 8 onward, with no evidence of detectable phage amplification. Fluorescence microscopy indicated greater membrane permeabilization in phage-treated microcosms at higher salinity. The microbial community remained dominated by Proteobacteria, particularly *Halomonas*. Overall, phage cocktail application coincided with a temporary and reversible decline in ammonia removal, particularly at higher salinity, emphasizing the need to evaluate its compatibility with essential biological treatment functions before practical implementation.

Keywords: bacteriophages; salinity; activated sludge; microbial community; biocontrol; 16S rRNA gene

Check for updates

Academic Editor: Martin Koller

Received: 24 September 2026
Revised: 22 October 2026
Accepted: 27 October 2026
Published: 30 October 2026

Copyright: © 2026 by the authors. Licensee MDPI, Basel, Switzerland. This article is an open access article distributed under the terms and conditions of the Creative Commons Attribution (CC BY) license.

1. Introduction

Produced water is the largest-volume wastewater generated during oil and gas production, and its management remains a major environmental and operational challenge for the petroleum industry [1–3]. Its variable composition includes dissolved salts, hydrocarbons, metals, process additives, and nitrogen compounds, which complicate treatment and may constrain discharge and reuse [1–5]. Ammonia removal is particularly challenging in highly saline produced water because osmotic stress can impair microbial activity and compromise biological treatment performance [6].

Biological nitrogen removal depends on microbial groups that differ in their metabolic capabilities and sensitivity to environmental conditions [6,7]. Alongside conventional autotrophic nitrification and heterotrophic denitrification, heterotrophic nitrification coupled with aerobic denitrification may contribute to nitrogen transformations in aerated systems supplied with organic carbon [8–12]. Physiological and genomic studies of bacteria isolated from petroleum wastewater have revealed diverse nitrogen-related metabolic repertoires [9,10,13]. Maintaining ammonia removal under saline conditions therefore requires communities adapted to the treatment matrix, whose activity and composition may change with increasing salinity [6,14,15].

Bacteriophages have been investigated as targeted bacterial control agents in environmental and industrial applications [16–20]. Their host specificity offers the potential to control undesirable bacteria while limiting direct effects on nonsusceptible microorganisms [17,18]. This approach is relevant to petroleum systems, where biofilm-forming and sulfate-reducing populations may contribute to hydrogen sulfide production and microbiologically influenced corrosion [21,22]. Bacteriophages and phage-encoded enzymes have consequently been investigated for biofilm control, while cocktails combining different phages may broaden coverage against target populations and reduce the likelihood of resistance [18,19,23–25].

However, host specificity alone does not ensure compatibility with essential microbial treatment functions. Phage-mediated changes in susceptible populations may alter substrate availability, microbial interactions, and community composition, with possible indirect consequences for nonsusceptible microorganisms [20,26,27]. Bacteriophages are abundant and diverse in activated sludge [28,29], and metagenomic studies have identified associations between viruses and microorganisms involved in carbon, nitrogen, and phosphorus removal [30]. These findings highlight the need to evaluate operational effects alongside the intended benefits of phage-based biocontrol.

Little is known about the consequences of intentionally applying phage cocktails to microbial communities treating highly saline oilfield produced water. In particular, it remains unclear whether a cocktail propagated using bacterial hosts not commonly associated with nitrification could affect ammonia removal or whether the response would differ between salinity conditions. Addressing this question is relevant to assessing the compatibility of industrial phage applications with downstream biological treatment.

To address this knowledge gap, this study evaluated whether a phage cocktail propagated using bacterial hosts not commonly associated with nitrification could affect ammonia removal by a microbial community treating oilfield produced water. The novelty of this study lies in assessing the compatibility of a phage cocktail intended for industrial biocontrol with an essential biological treatment function in a complex microbial community acclimated to highly saline produced water. A single dose of the phage cocktail, at a final concentration of 10^7 PFU mL^{-1}, was applied to microcosms containing sludge previously acclimated to 55 and 125 g L^{-1} NaCl. Operational and microbiological responses were assessed by jointly monitoring ammonia removal, infective bacteriophage persistence, qualitative changes in cell membrane integrity, and prokaryotic community composition. We hypothesized that the phage cocktail would not impair ammonia removal because the bacterial hosts used for phage propagation were not among the main microbial groups associated with nitrification in the treatment system. The two salinity conditions were evaluated to assess whether the magnitude and duration of the response to cocktail application differed between salinity levels.

2. Materials and Methods

2.1. Phage Cocktail

The cocktail comprised the bacteriophages vB_EcoM-UFV09, vB_EcoM-UFV10, and vB_EcoM-UFV13, isolated using *Escherichia coli* as the host, and vB_EclM-UFV01, isolated using *Enterobacter cloacae*. The phages belong to the Bacterial Virus Collection of the Laboratory of Molecular Immunovirology at the Federal University of Viçosa (Brazil). Their genome sequences are available in the NCBI database under accession numbers MZ291552.2, OP555981.1, KU867876.1, and ON454249, respectively.

The cocktail was originally formulated for biofilm control on metal surfaces associated with petroleum-industry operations. The four phages, described as lytic by Vieira et al. [31], were selected based on their demonstrated ability to disrupt sulfate-reducing bacterial biofilms, together with considerations of industrial applicability and production scale-up. Before cocktail preparation, each phage underwent individual host-range assessment, evaluation of plaque-forming activity, biofilm-inhibition screening, and genomic characterization [31].

The phages were produced separately in 5 L bioreactors containing Luria–Bertani medium composed of 10 g L^{-1} NaCl, 10 g L^{-1} peptone, and 5 g L^{-1} yeast extract. Cultures were incubated for 5 h at 30 °C under agitation. Subsequently, the cultures were centrifuged at 8000× *g* for 10 min, and the supernatants were filtered through 0.22 µm membranes. The phage suspensions were titrated using a plaque assay and stored at 4 °C for up to three months.

A single final cocktail concentration of 10^7 PFU mL^{-1} in the microcosms was selected for consistency with the concentration evaluated in the associated pilot-scale biocontrol study by Vieira et al. [31]. The present study focused on evaluating the response of produced-water treatment communities to a single application at this concentration, rather than establishing an optimal dose. Concentration-dependent effects were not experimentally evaluated; therefore, the findings are restricted to the tested concentration and application regime.

2.2. Microcosm Experimental Design and Operation

The sludge was obtained from an industrial biological treatment system for produced water at an oil terminal and was previously acclimated in sequential batches using produced water with increasing NaCl concentrations [6]. Sludge acclimated to 55 and 125 g L^{-1} NaCl was evaluated. These salinities were selected to represent two operational scenarios. A NaCl concentration of 55 g L^{-1} was representative of the produced water received by the industrial treatment system investigated, whereas 125 g L^{-1} represented a potential hypersaline scenario associated with produced water from pre-salt reservoirs. The higher salinity was also selected based on previous studies demonstrating that acclimated microbial communities could maintain ammonia removal under these conditions.

For each salinity, four microcosms were established in Erlenmeyer flasks with a working volume of 250 mL and a 10% inoculum. Two microcosms were maintained as controls, while the other two received a single dose of the phage cocktail at a final concentration of 10^7 PFU mL^{-1}. The microcosms were incubated at 30 °C and 150 rpm.

The microcosms were fed once daily, six days per week. Before each feeding, agitation was stopped, and the sludge was allowed to settle for 1 h. Subsequently, approximately 18% of the working volume was withdrawn and replaced with produced water containing 80 mg L^{-1} ammonia, 1.5 mL L^{-1} ethanol, and 2.5 mL L^{-1} tripolyphosphate. Microcosms containing 125 g L^{-1} NaCl also received 1.5 g L^{-1} $NaHCO_3$ to maintain residual alkalinity above 300 mg L^{-1}. Before application of the phage cocktail, the systems were stabilized for at least 30 days until ammonia removal exceeded 90%. All experimental conditions were evaluated in duplicate.

2.3. Ammonia and Bacteriophage Quantification

Ammonia concentration was determined using the phenol-hypochlorite colorimetric method described by Chaney and Marbach [32] and modified by Zhang et al. [33]. In 96-well microplates, 5 µL of each sample was mixed with 100 µL of phenol reagent and 100 µL of hypochlorite reagent. After incubation at 39 °C for 20 min, absorbance was measured at 630 nm using a Multiskan GO microplate spectrophotometer (Thermo Scientific, Wilmington, DE, USA). Ammonia removal efficiency was calculated from the difference between the influent and effluent concentrations relative to the influent concentration [9].

Infective bacteriophages in the phage-treated microcosms were quantified using a double-layer agar plaque assay, with *E. coli* and *E. cloacae* as indicator bacteria. Briefly, appropriate sample dilutions were mixed with the corresponding bacterial host and molten soft agar. The mixture was then poured over a solid agar layer and incubated until visible plaques were formed. Plaques were counted, and phage titers were calculated considering the number of plaques, dilution factor, and plated volume. Results were expressed as plaque-forming units per milliliter (PFU mL^{-1}). Titers obtained using *E. coli* represented vB_EcoM-UFV09, vB_EcoM-UFV10, and vB_EcoM-UFV13 collectively, whereas titers obtained using *E. cloacae* represented vB_EclM-UFV01.

2.4. Assessment of Cell Membrane Integrity

Cell membrane integrity was qualitatively assessed using the LIVE/DEAD BacLight™ Bacterial Viability Kit (L7012, Invitrogen, Thermo Fisher Scientific), according to the manufacturer's instructions. Samples were stained with SYTO 9 and propidium iodide and examined using an EVOS M5000 fluorescence imaging system (Invitrogen, Thermo Fisher Scientific). Cells exhibiting predominantly green fluorescence were interpreted as having intact membranes, whereas cells exhibiting red or orange fluorescence were considered to have compromised membranes.

2.5. Microcosm DNA Extraction

Total microbial community DNA was extracted from 1 mL of microcosm according to Silva et al. [9], with modifications. Samples were washed seven times with SET buffer and subjected to enzymatic lysis with lysozyme and proteinase K, followed by SDS treatment and three cycles of freezing in liquid nitrogen and thawing at 65 °C. DNA was purified with phenol and chloroform:isoamyl alcohol (24:1), precipitated with NaCl and absolute ethanol, washed with 70% ethanol, and resuspended in 25 µL of Milli-Q water. DNA integrity was assessed by electrophoresis on a 1% agarose gel stained with GelRed® (Biotium, Fremont, CA, USA), while DNA concentration and purity were determined using a NanoDrop ND-1000 spectrophotometer (Thermo Fisher Scientific, Wilmington, DE, USA).

2.6. 16S rRNA Gene Sequencing and Bioinformatic Analysis

Samples for 16S rRNA gene sequencing were collected at the end of the experiment, 55 days after phage cocktail application. Two biological replicates were sampled for each treatment–salinity combination (control and phage-treated microcosms at 55 and 125 g L^{-1} NaCl), yielding eight biological samples in total.

The V3–V4 region of the 16S rRNA gene was amplified and sequenced on an Illumina platform using paired-end reads. Raw-read quality was assessed using FastQC version 0.11.5. Sequence processing was performed in R using DADA2 version 1.38.0. The pipeline included quality filtering (maxN = 0, maxEE = c(2, 2), truncQ = 2, and rm.phix = TRUE), error-rate learning, dereplication, inference of amplicon sequence variants (ASVs), merging of paired-end reads with a minimum overlap of 12 bp, and chimera removal.

Taxonomic assignment was performed against the SILVA reference database, version 138.1, using a minimum bootstrap confidence threshold of 80%. The resulting ASV abundance and taxonomic tables were imported into the phyloseq package for downstream analysis. Sequencing coverage was examined using rarefaction curves, and alpha diversity was characterized using observed ASV richness and the Shannon and Simpson diversity indices. Taxonomic composition was evaluated at the phylum and genus levels and expressed as relative abundance.

2.7. Statistical Analysis

Ammonia removal efficiencies and infective phage titers obtained from duplicate microcosms were expressed as the mean and standard deviation. Differences in ammonia removal between control and phage cocktail-treated microcosms were evaluated separately at each sampling time using two-sided independent-samples *t*-tests. The resulting *p*-values were adjusted separately within each salinity condition using the Holm method to account for multiple comparisons. Holm-adjusted *p*-values ≤ 0.05 were considered statistically significant.

3. Results

3.1. Effect of the Phage Cocktail on Ammonia Removal

Before the application of the phage cocktail, all microcosms exhibited high ammonia removal efficiencies, with mean values ranging from 94.50% to 98.50% (Figure 1). No significant differences were observed between the control and treated microcosms on day 0 at either 55 or 125 g L^{-1} NaCl. Throughout the experimental period, the controls remained stable, maintaining removal efficiencies above 94% at both salinities. In contrast, the application of the phage cocktail was followed by a temporary reduction in ammonia removal, the magnitude and duration of which differed between the salinity conditions. Detailed pairwise statistical comparisons are presented in Appendix A (Table A1).

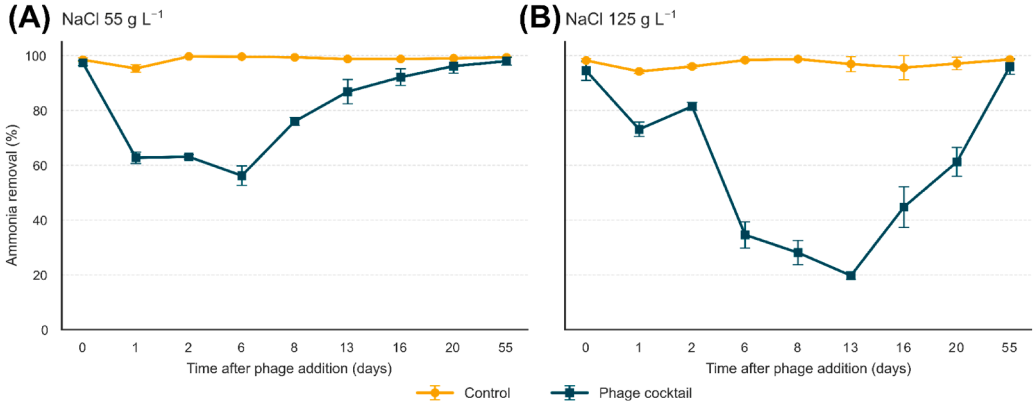


Figure 1. Ammonia removal efficiency in control and phage-treated microcosms operated at 55 g L^{-1} (**A**) and 125 g L^{-1} NaCl (**B**). The phage cocktail was applied once on day 0 at a final concentration of 10^7 PFU mL^{-1}. Values represent the mean ± standard deviation of duplicate microcosms ($n = 2$). For clarity, sampling times are displayed at equally spaced positions; labels indicate the actual days after phage cocktail application.

In the microcosms maintained at 55 g L^{-1} NaCl, the mean removal efficiency decreased from 97.35 ± 0.92% on day 0 to 62.78 ± 2.09% on the first day after cocktail application. Ammonia removal remained close to 63% on day 2 and reached its lowest value on day 6, at 56.22 ± 3.57%, whereas the control exhibited an efficiency of 99.65 ± 0.07%. Differences between the treatments were significant on days 1, 2, 6, and 8 after Holm correction (adjusted

$p \leq 0.020$). From day 8 onward, ammonia removal progressively recovered, increasing to 86.85 ± 4.45% on day 13 and 92.15 ± 3.04% on day 16. Differences relative to the control were no longer significant from day 13 onward. On day 55, the treated microcosms exhibited a removal efficiency of 98.00 ± 1.41%, close to the 99.40 ± 0.14% observed in the controls.

The reduction in ammonia removal was more pronounced and persistent in the microcosms maintained at 125 g L^{-1} NaCl. Following cocktail application, the removal efficiency decreased from 94.50 ± 3.54% on day 0 to 73.12 ± 2.65% on day 1. Although it increased to 81.50 ± 1.41% on day 2, ammonia removal declined again at the subsequent sampling times, reaching 34.62 ± 4.77% on day 6 and 28.12 ± 4.42% on day 8. The lowest value was recorded on day 13, when only 19.75 ± 1.41% of the ammonia was removed, compared with 96.94 ± 2.74% in the control. Significant differences between the treatments were observed on days 1, 2, 6, 8, and 13, with adjusted *p*-values ranging from 0.007 to 0.042.

Recovery of the treated microcosms at 125 g L^{-1} NaCl began after day 13, with removal efficiency increasing to 44.75 ± 7.42% on day 16 and 61.25 ± 5.30% on day 20. Despite the numerically large differences relative to the controls at these two sampling times, they did not remain significant after Holm correction (adjusted $p = 0.051$). Recovery to values above 90% was observed only on day 55, when removal efficiency reached 96.00 ± 2.83%, compared with 98.62 ± 0.18% in the controls.

Overall, the results show that a single application of the phage cocktail was associated with a transient reduction in ammonia removal. At 55 g L^{-1} NaCl, the effect was less pronounced, and removal above 90% was restored by day 16. At 125 g L^{-1} NaCl, the loss of efficiency was more severe, and recovery above 90% occurred only on day 55, indicating a more persistent operational impact under the higher-salinity condition.

3.2. Dynamics of Infective Bacteriophages Following Phage Cocktail Application

Immediately after cocktail application, infective bacteriophages were recovered from all treated microcosms (Figure 2). Titers determined using *E. coli* ranged from approximately 3.2×10^6 to 6.6×10^6 PFU mL^{-1}, whereas those determined using *E. cloacae* ranged from 9.7×10^5 to 3.8×10^6 PFU mL^{-1}. Thus, the initial infective phage titers were close to the applied cocktail concentration, although the values obtained with *E. cloacae* were generally lower than those determined with *E. coli*.

A pronounced reduction in infective phage titers was observed on day 6. Using *E. coli* as the indicator bacterium, titers decreased to values ranging from approximately 1.0×10^1 to 6.9×10^2 PFU mL^{-1}, corresponding to a reduction of approximately four to six orders of magnitude relative to the initial titers. At the same sampling time, no infective phages were recovered using *E. cloacae* as the indicator bacterium. From day 8 onward, no infective bacteriophages were detected with either indicator bacterium, and this condition persisted until the final sampling on day 19.

No increase in infective phage titers was observed at either salinity. Instead, the results demonstrated a rapid loss of the phage fraction capable of forming plaques on the indicator strains, with no evidence of detectable amplification in the microcosms. Because the assay performed with *E. coli* collectively quantified phages vB_EcoM-UFV09, vB_EcoM-UFV10, and vB_EcoM-UFV13, the persistence of each bacteriophage could not be evaluated separately. In contrast, the results obtained with *E. cloacae* corresponded to phage vB_EclM-UFV01.

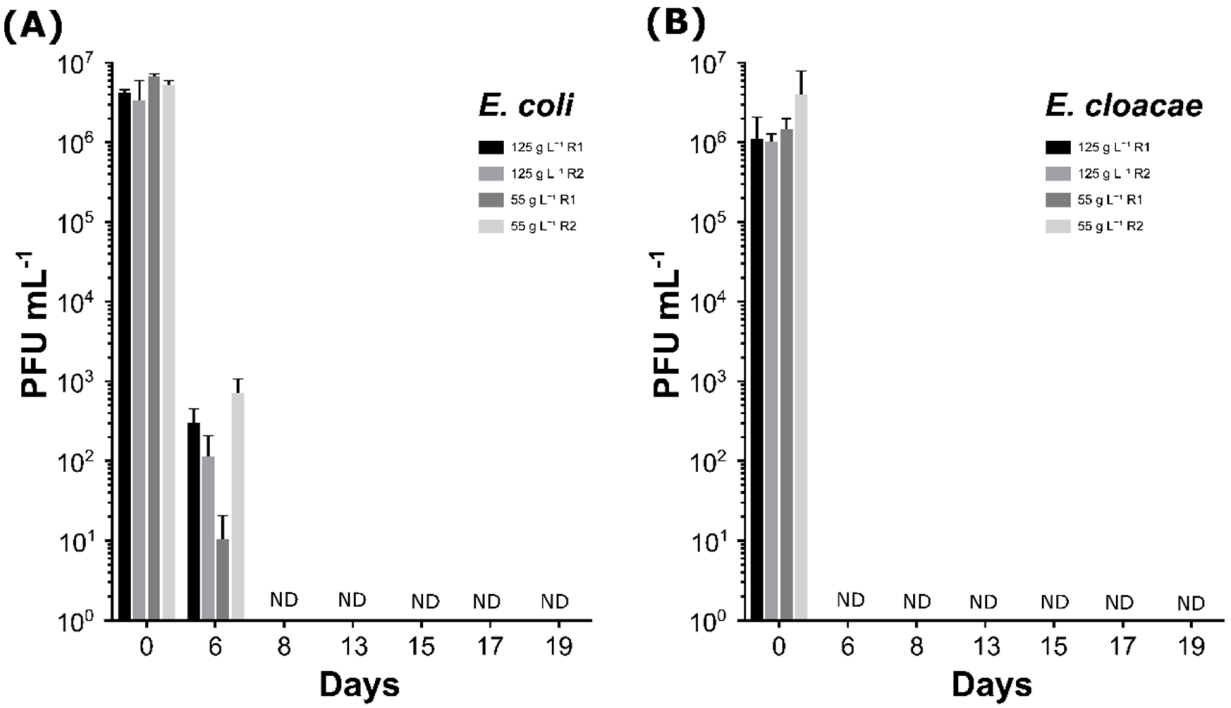


Figure 2. Dynamics of infective bacteriophages over 19 days following phage cocktail application, determined by the double-layer agar plaque assay using *Escherichia coli* (**A**) and *Enterobacter cloacae* (**B**) as indicator bacteria. Bars represent individual biological replicate microcosms maintained at 55 or 125 g L^{-1} NaCl. Values are means of three technical determinations, and error bars indicate standard deviations. ND indicates that no plaques were detected in any replicate microcosm at the corresponding sampling time. Titers obtained using *E. coli* represent vB_EcoM-UFV09, vB_EcoM-UFV10, and vB_EcoM-UFV13 collectively, whereas those obtained using *E. cloacae* correspond to vB_EclM-UFV01.

3.3. Qualitative Assessment of Cell Membrane Integrity

Staining with SYTO 9 and propidium iodide revealed distinct fluorescence patterns among the experimental conditions (Figure 3). In the control microcosms maintained at 55 and 125 g L^{-1} NaCl, microbial aggregates exhibited predominantly green fluorescence, indicating the predominance of cells with intact membranes in the examined fields.

In the microcosms treated with the phage cocktail at 55 g L^{-1} NaCl, green fluorescence also predominated, accompanied by occasional red and orange signals. Thus, no widespread impairment of cell membrane integrity was observed under this condition.

A different pattern was observed in the treated microcosms maintained at 125 g L^{-1} NaCl. Although green fluorescence remained present, the aggregates exhibited more conspicuous red and orange signals distributed across different regions. The simultaneous occurrence of both fluorescence patterns indicated the presence of cells with intact and compromised membranes within the same aggregate and suggested greater membrane impairment under this condition.

Because the assessment was qualitative and based on representative microscopic fields, the proportion of cells with intact or compromised membranes could not be determined. Nevertheless, the images indicated that the most pronounced pattern of membrane impairment occurred in microcosms simultaneously exposed to the phage cocktail and the highest NaCl concentration.

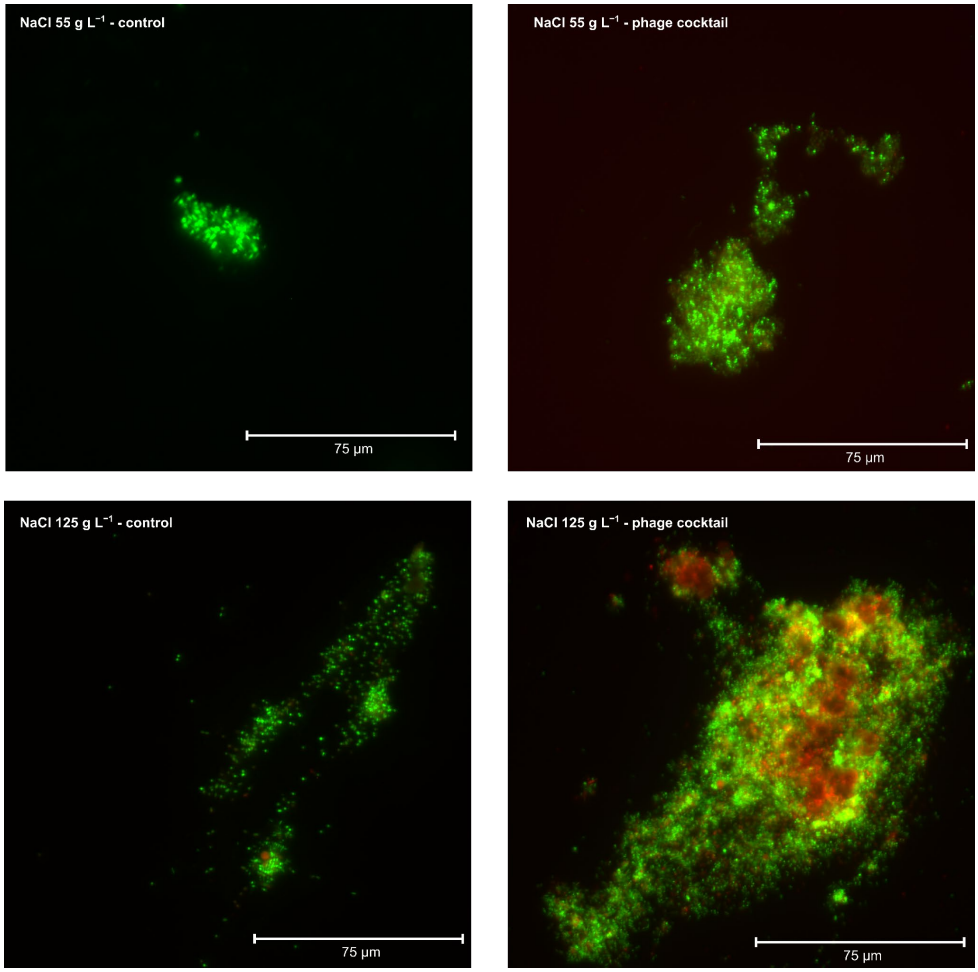


Figure 3. Qualitative assessment of cell membrane integrity in control and phage cocktail-treated microcosms. Representative fluorescence microscopy images of microbial aggregates from microcosms maintained at 55 g L^{-1} NaCl, control and phage cocktail, and at 125 g L^{-1} NaCl, control and phage cocktail. Samples were stained using the LIVE/DEAD BacLight™ Bacterial Viability Kit. Green fluorescence indicates cells with predominantly intact membranes, whereas red or orange fluorescence indicates cells with compromised membranes. Images were acquired using an EVOS M5000 fluorescence imaging system. Scale bars: 75 µm.

3.4. Sequencing Coverage and Alpha Diversity

After sequence processing, the samples included in the main analysis contained between 114,030 and 128,320 reads, yielding a total of 5192 ASVs. The rarefaction curves approached a plateau at the highest sequencing depths, indicating that the sequencing effort adequately captured most of the observed richness.

ASV richness ranged from 480 to 1931 across samples. At 55 g L^{-1} NaCl, the mean richness values were similar between the control and phage cocktail treatments, with 1058.5 and 1055.5 ASVs, respectively. A similar pattern was observed for the Shannon index, with values of 3.119 and 3.068, and for the Simpson index, with values of 0.800 and 0.798, respectively.

At 125 g L^{-1} NaCl, 709 ASVs were detected in the control condition and 1931 ASVs in the phage cocktail treatment. The corresponding Shannon index values were 3.822 and 4.432, whereas the Simpson index values were 0.953 and 0.898, respectively. These findings revealed variation in richness and abundance distribution among samples, although the diversity metrics did not exhibit a consistent pattern.

3.5. Microbial Composition of the Microcosms

The prokaryotic community was predominantly composed of members of Proteobacteria under all evaluated conditions (Figure 4A). This phylum accounted for approximately 85% of the relative abundance in microcosms maintained at 55 g L^{-1} NaCl and approximately 70% in those maintained at 125 g L^{-1} NaCl. Therefore, although its relative contribution was lower at the higher salinity, Proteobacteria remained the dominant phylum regardless of phage cocktail application.

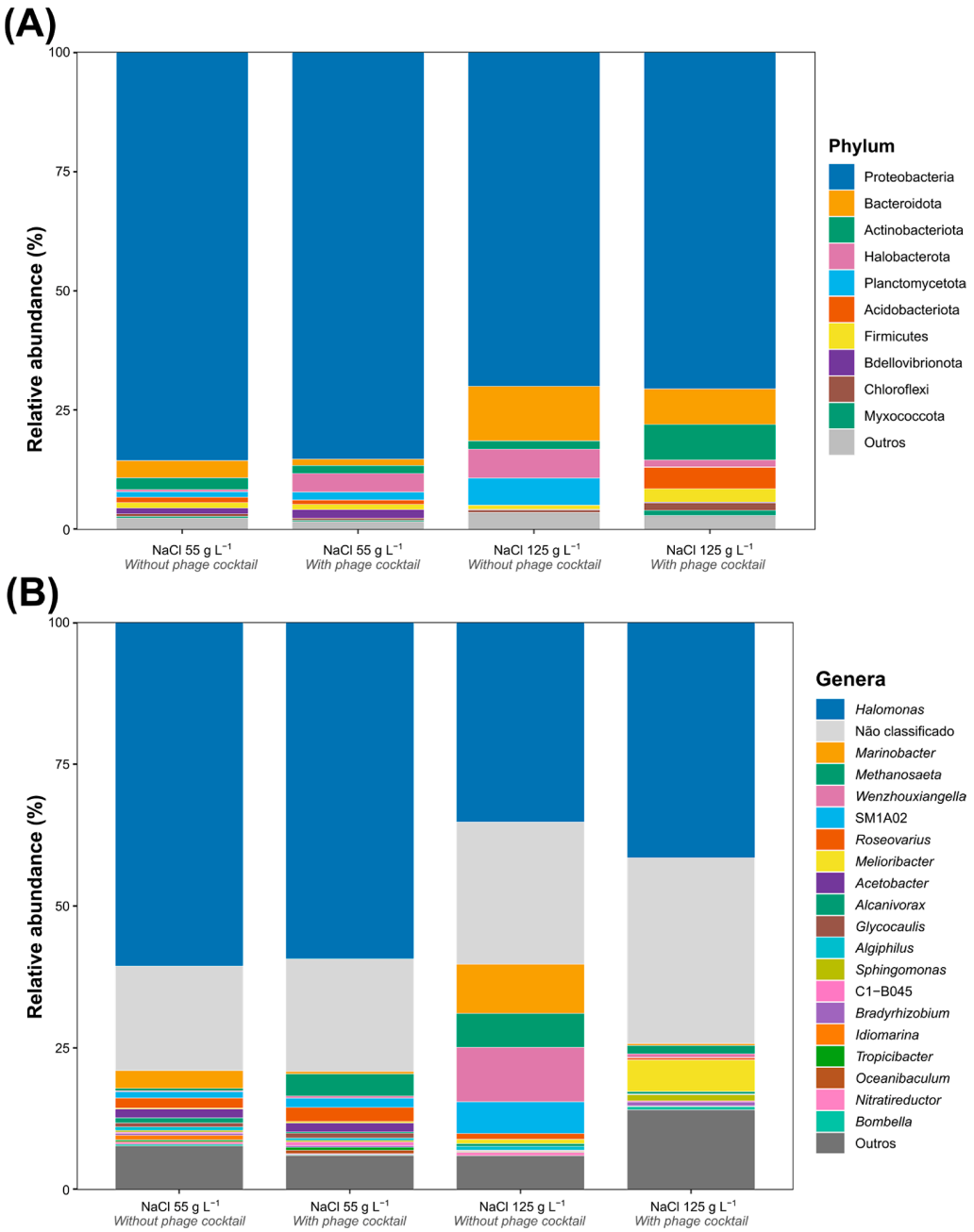


Figure 4. Prokaryotic community composition in control and phage cocktail-treated microcosms maintained at 55 or 125 g L^{-1} NaCl. (**A**) Relative abundance of prokaryotic phyla. (**B**) Relative abundance of the predominant prokaryotic genera. Taxonomic composition was determined by sequencing the V3–V4 region of the 16S rRNA gene. In panel (**A**), each stacked bar represents the relative abundance of the detected phyla within each experimental condition. In panel (**B**), colors and numerical values indicate the relative abundance (%) of each genus.

At 55 g L^{-1} NaCl, the taxonomic profiles were similar between the control and phage cocktail treatments. In addition to Proteobacteria, Bacteroidota, Actinobacteriota, Halobacterota, Planctomycetota, Acidobacteriota, Firmicutes, Bdellovibrionota, Chloroflexi, and Myxococcota were detected, all at considerably lower relative abundances. Differences between treatments at this salinity were mainly restricted to the less abundant phyla and did not substantially modify the overall community structure at the phylum level.

Greater variation in the contribution of less abundant phyla was observed at 125 g L^{-1} NaCl. At this salinity, Bacteroidota, Halobacterota, and Planctomycetota showed higher relative abundances in the control condition. Conversely, Actinobacteriota, Acidobacteriota, and Firmicutes were comparatively more abundant in the phage cocktail-treated condition. Despite these variations, Proteobacteria remained dominant under both conditions.

Overall, the results indicated that salinity was associated with the most evident differences in community composition at the phylum level. The predominance of Proteobacteria was maintained following phage cocktail application, although variations in the relative contributions of less abundant phyla were observed, particularly at 125 g L^{-1} NaCl.

The genus-level analysis revealed the predominance of *Halomonas* under all experimental conditions (Figure 4B). At 55 g L^{-1} NaCl, this genus represented 60.58% of the community in the control and 59.30% in the phage cocktail treatment. At 125 g L^{-1} NaCl, its relative abundance was lower, accounting for 35.21% in the control and 41.51% in the phage cocktail-treated condition. These results show that the high relative abundance of *Halomonas* was maintained following phage cocktail application, although its contribution varied with salinity.

Sequences that could not be classified at the genus level constituted the second-largest fraction of the community under all four conditions and made a greater contribution for the microcosms maintained at 125 g L^{-1} NaCl. This fraction indicates that a substantial proportion of sequences, particularly under the higher-salinity condition, could not be assigned to the genera represented in the reference database at the confidence threshold adopted.

Among the other genera, *Marinobacter* showed a relative abundance of 3.12% in the control and 0.46% in the phage cocktail treatment at 55 g L^{-1} NaCl. At 125 g L^{-1} NaCl, this genus accounted for 8.68% of the control community and 0.35% of the phage cocktail-treated community. Thus, the highest contribution of *Marinobacter* was observed in the control maintained at the higher salinity.

Roseovarius represented 1.76% and 2.48% of the control and phage cocktail-treated communities, respectively, at 55 g L^{-1} NaCl. At 125 g L^{-1} NaCl, its relative abundance was 1.03% in the control and 0.37% in the phage cocktail treatment. *Nitratireductor*, in turn, accounted for 0.31% and 0.18% at 55 g L^{-1} NaCl and 0.62% and 0.02% at 125 g L^{-1} NaCl in the control and phage cocktail treatments, respectively.

Other genera also contributed to the differences observed at the higher salinity. The control at 125 g L^{-1} NaCl showed greater contributions from *Wenzhouxiangella*, *Methanosaeta*, and SM1A02, in addition to *Marinobacter*. In the phage cocktail-treated condition, *Melioribacter* and taxa grouped within the "Other" category made greater contributions. Genera such as *Acetobacter*, *Alcanivorax*, *Glycocaulis*, *Algiphilus*, *Sphingomonas*, *Bradyrhizobium*, *Idiomarina*, *Tropicibacter*, *Oceanibaculum*, and *Bombella* were also detected, but at lower relative abundances.

Overall, the genus-level profiles were more similar between treatments at 55 g L^{-1} NaCl, particularly because of the comparable predominance of *Halomonas*. At 125 g L^{-1} NaCl, more evident differences were observed in the contributions of less abundant genera and the unclassified fraction. However, these variations did not show a consistent pattern of enrichment or reduction associated with the phage cocktail, and *Halomonas* remained the predominant genus under all conditions.

3.6. Genera Potentially Associated with Nitrogen Transformations

Genera previously described in the literature, such as those associated with different stages of the nitrogen cycle, including autotrophic nitrification, heterotrophic nitrification, and denitrification, were detected (Figure 5). Among the observed genera, *Halomonas* exhibited the highest relative abundances under all conditions, ranging from 35.21% to 60.58%. At 55 g L^{-1} NaCl, its abundance was similar in the control and phage cocktail treatments, corresponding to 60.58% and 59.30%, respectively. At 125 g L^{-1} NaCl, the corresponding values were 35.21% in the control and 41.51% in the presence of the phage cocktail.

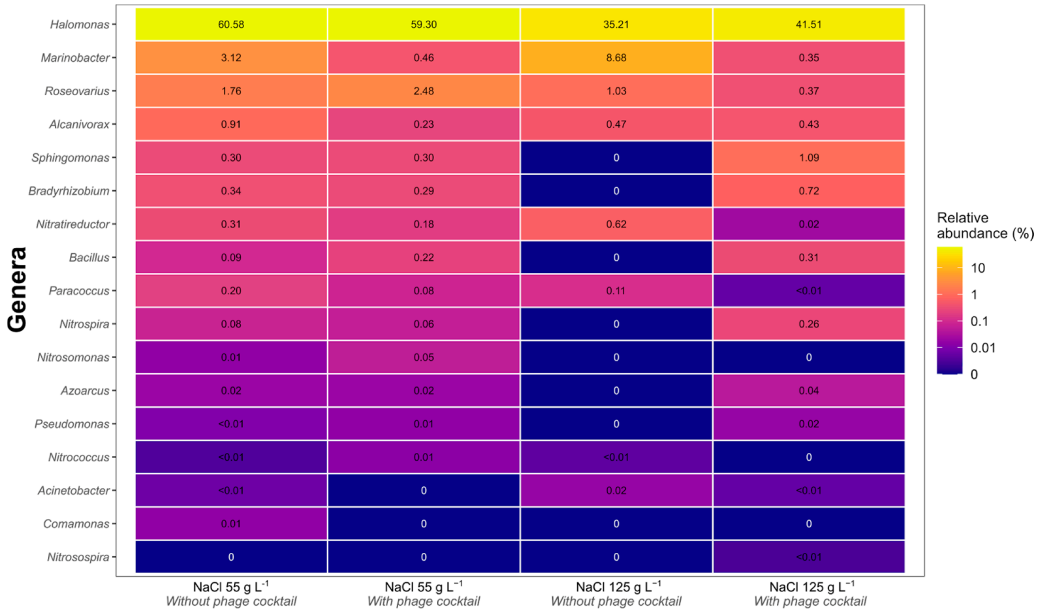


Figure 5. Relative abundance of genera potentially associated with nitrogen transformations in control and phage cocktail-treated microcosms. Columns correspond, from left to right, to control and phage cocktail-treated microcosms maintained at 55 g L^{-1} NaCl, followed by control and treated microcosms maintained at 125 g L^{-1} NaCl. Cell values indicate the relative abundance of each genus as a percentage of the prokaryotic community, and the color scale represents increasing relative abundance. Values below 0.01% are shown as <0.01, whereas zero indicates that the genus was not detected.

Other genera potentially associated with heterotrophic nitrification and aerobic denitrification were detected at lower relative abundances. *Marinobacter* accounted for 3.12% and 0.46% at 55 g L^{-1} NaCl and 8.68% and 0.35% at 125 g L^{-1} NaCl in the control and phage cocktail treatments, respectively. The relative abundance of *Roseovarius* ranged from 0.37% to 2.48%, whereas that of *Alcanivorax* ranged from 0.23% to 0.91%.

Sphingomonas and *Bradyrhizobium* showed similar relative abundances between treatments at 55 g L^{-1} NaCl, ranging from 0.29% to 0.34%. At 125 g L^{-1} NaCl, these genera were not detected in the control but accounted for 1.09% and 0.72%, respectively, in the phage cocktail-treated condition. *Bacillus* was also not detected in the control at 125 g L^{-1} NaCl but represented 0.31% of the community in the presence of the cocktail. In contrast, the relative abundance of *Nitratireductor* decreased from 0.62% in the control to 0.02% in the phage cocktail-treated condition at this salinity.

Paracoccus was detected under all conditions, although at low relative abundances ranging from less than 0.01% to 0.20%. *Azoarcus*, *Pseudomonas*, *Acinetobacter*, and *Comamonas* also exhibited low relative abundances or were restricted to specific conditions. *Azoarcus* ranged from 0.02% to 0.04%, whereas *Pseudomonas*, *Acinetobacter*, and *Comamonas* did not exceed 0.02%.

Genera associated with autotrophic nitrification represented a small fraction of the community. *Nitrospira* was detected at relative abundances of 0.08% and 0.06% in the control and phage cocktail treatments, respectively, at 55 g L^{-1} NaCl. At 125 g L^{-1} NaCl, this genus was not detected in the control but represented 0.26% of the community in the presence of the cocktail. *Nitrosomonas* accounted for 0.01% in the control and 0.05% in the phage cocktail treatment at 55 g L^{-1} NaCl but was not detected under either condition at 125 g L^{-1} NaCl. *Nitrococcus* occurred at relative abundances equal to or below 0.01%, whereas *Nitrosospira* was detected only in the phage cocktail-treated condition at 125 g L^{-1} NaCl, at an abundance below 0.01%.

Overall, the results showed that the microbial community contained various genera specifically associated with nitrification processes, with a marked predominance of *Halomonas* and low representation of classical autotrophic nitrifiers. However, the application of the phage cocktail did not result in the widespread disappearance of these groups, although specific variations in their abundance were observed across different salinities.

4. Discussion

Application of the phage cocktail was associated with a temporary disturbance in ammonia removal, with a more persistent response under the highest salinity condition. Operational effects related to phage activity have previously been reported in biological treatment systems. Barr et al. [34] associated infection of Candidatus *Accumulibacter* with deterioration of phosphorus removal, whereas Shapiro et al. [35] observed temporal relationships between phage titers and the abundance of bacterial groups in an industrial bioreactor. Regarding nitrogen metabolism, Liao et al. [36] demonstrated that infection of a bacterium capable of heterotrophic nitrification and aerobic denitrification impaired ammonia removal. The present study documents a transient decline in ammonia removal following cocktail application to a complex microbial community acclimated to saline produced water. Unlike studies demonstrating infection of specific functional populations, the present results do not establish direct infection of ammonia-removing microorganisms. The interpretation therefore requires consideration of salinity, infective phage persistence, membrane integrity, and the microbial community observed at the experimental endpoint.

The more persistent response at 125 g L^{-1} NaCl may be related to a reduced physiological capacity of the community to withstand an additional disturbance. Acclimation can support nitrification under saline conditions, but it does not eliminate the energetic costs associated with osmoregulation, ion transport, and the synthesis or uptake of compatible solutes [6,37–39]. Campos et al. [39] reported greater salt tolerance in adapted biomass, although specific nitrifying activity still decreased as salinity increased. Bassin et al. [40] also found that acclimation favored nitrification in saline wastewater but did not completely prevent inhibition by other matrix components. Changes in nitrification and denitrification rates and in mechanisms of ionic homeostasis under increasing salinity were also reported by Liu et al. [38]. Thus, the high efficiency maintained by the controls demonstrates adaptation to the operating conditions but does not necessarily imply an equivalent capacity to withstand a new disturbance.

From an ecological perspective, ammonia removal recovered more rapidly at 55 g L^{-1} NaCl than at 125 g L^{-1} NaCl. This difference can be interpreted in terms of functional recovery following disturbance [41]. Restoration of a function, however, does not necessarily require the microbial community to return to its initial structure. Vuono et al. [42] observed recovery of nutrient removal processes after disturbance despite incomplete restoration of bacterial diversity. Santillan et al. [43] likewise showed that nitrification can be restored by populations other than those that were initially dominant. In the present system, re-

covery of ammonia removal may have involved the growth of nonsusceptible populations, adaptation of surviving cells, or replacement of affected groups by functionally redundant microorganisms [40–43].

There is no evidence that the functional response resulted from direct infection of the principal nitrifying groups. *E. coli* and *E. cloacae* were not among the dominant taxa or the main genera associated with nitrogen metabolism. Nevertheless, phages isolated from activated sludge may infect different strains, species, or genera [28,43]. Lysis of susceptible populations may also alter substrate availability, metabolic interactions, and aggregate organization, thereby indirectly affecting functions performed by other microbial groups [33–36]. Distinguishing among these mechanisms would require host-range assays with isolates obtained from the sludge, absolute quantification of microbial populations, and temporal monitoring of community composition.

The absence of an increase in infective titers indicates that no detectable amplification of the cocktail components occurred. Viral propagation requires permissive and metabolically active hosts at sufficient densities. Even in sludge containing a high total viral abundance, only a fraction of the phages may form plaques on the culturable bacteria used as indicators [34,35,44]. The decline in infectivity may have resulted from the absence of suitable hosts, loss of particle stability, or association of the phages with solids, organic matter, and the extracellular matrix of the flocs [35,45]. Salinity, pH, temperature, and ionic composition may also affect adsorption to bacterial receptors and infection efficiency [45].

Plaque assays detect only particles capable of completing a lytic cycle in the indicator strains under the conditions employed. Therefore, the absence of plaques indicates a loss of detectable infectivity rather than necessarily the physical elimination of phage particles [44,45]. This distinction is relevant because ammonia removal recovered after infective phages were no longer detected, particularly at higher salinity. An initial exposure may have triggered population-level or physiological changes that persisted after the infective viral fraction declined [34,35]. Consequently, monitoring phage titers in the liquid phase alone may not adequately represent the duration of the functional response of a system exposed to phage-based biocontrol.

The greater occurrence of red and orange fluorescence in the phage-treated microcosms at 125 g L^{-1} NaCl suggests increased membrane permeabilization in the examined fields. However, this observation cannot be attributed specifically to direct phage infection. Although the controls exhibited predominantly green fluorescence, the pattern observed in treated microcosms may reflect combined physiological stress associated with cocktail application under hypersaline conditions. Osmotic stress may increase the physiological burden on acclimated communities and reduce their capacity to withstand an additional disturbance [37–39]. The SYTO 9/propidium iodide staining system assesses membrane integrity, which is not necessarily equivalent to metabolic activity or growth capacity [46–50]. Staining may also be influenced by cellular physiological state, aggregation, and extracellular nucleic acids within the flocs [46–50]. Therefore, these qualitative images neither quantify cell mortality nor identify the affected populations or establish the mechanism responsible for membrane damage.

The predominance of Proteobacteria is consistent with communities reported in treatment systems receiving petroleum-related and saline effluents [9,10,51–53]. Its predominance at day 55 is compatible with the selection of microorganisms adapted to saline produced water. However, because community composition was assessed only at the end of the experiment, these profiles cannot establish whether transient taxonomic changes occurred following cocktail application.

The predominance of *Halomonas* at the experimental endpoint is consistent with its adaptation to saline environments. Species belonging to this genus are frequently enriched

in saline bioreactors and possess osmoadaptation mechanisms, including compatible-solute synthesis and ion-homeostasis systems [51–55]. Different strains may also perform heterotrophic nitrification, aerobic denitrification, or ammonia assimilation under saline conditions [51,54,55]. In the present study, *Halomonas* was predominant in both control and phage-treated microcosms at day 55. However, these endpoint relative-abundance profiles cannot exclude an earlier decline or changes in its absolute abundance or metabolic activity. Previous studies have linked phage-associated disturbances to changes in microbial populations and community interactions [34,35]. Such processes may have contributed to the observed functional response, but the involvement of *Halomonas*, less abundant populations, or indirect microbial interactions could not be resolved in this study.

The low representation of *Nitrosomonas*, *Nitrospira*, *Nitrococcus*, and *Nitrosospira* suggests that ammonia removal did not depend exclusively on classical autotrophic nitrifiers. These groups may lose activity and competitive fitness under osmotic stress, although low-abundance populations can still make important functional contributions [14,37–39,52–57]. In contrast, several halotolerant genera associated in the literature with heterotrophic nitrification, aerobic denitrification, or ammonia assimilation were detected, including *Halomonas*, *Marinobacter*, *Paracoccus*, *Bacillus*, *Pseudomonas*, and *Acinetobacter* [8–13,51–55]. The simultaneous availability of ammonia, oxygen, and ethanol may have favored heterotrophic metabolism, but the decrease in ammonia concentration alone cannot distinguish its oxidation from incorporation into microbial biomass.

Taxonomic composition and treatment performance provide complementary information, but the endpoint profiles obtained here cannot explain the preceding functional decline. Changes in metabolic activity, gene expression, or absolute population sizes may affect ammonia removal without corresponding changes in relative taxonomic abundance [40–42,56–58]. Furthermore, species within the same genus may differ in their metabolic repertoires, so taxonomic detection alone does not confirm the presence or expression of specific nitrogen-transformation pathways [10,56,58]. Functional redundancy may have contributed to recovery, but this remains a hypothesis requiring temporal community analysis and functional measurements.

From an operational perspective, phage specificity alone is insufficient to establish compatibility with essential biological treatment functions. Assessments of industrial phage cocktails should integrate host range, persistence in the treatment matrix, and possible indirect effects on microbial communities [20,24,25,34,35]. The present findings are limited to one cocktail concentration and one application event; consequently, a dose–response relationship could not be established. Microscopy was qualitative, and the bacterial populations susceptible to infection within the sludge were not identified. Moreover, sequencing was performed only on day 55, preventing reconstruction of community changes during the initial disturbance and subsequent recovery. Future studies should combine temporal sampling, absolute quantification of functional populations, direct host-range assessment, and measurements of nitrogen-transformation pathways under representative operating conditions.

5. Conclusions

A single application of the phage cocktail at 10^7 PFU mL^{-1} was followed by a transient reduction in ammonia removal by produced-water-acclimated sludge, with faster recovery at 55 g L^{-1} NaCl and a more persistent effect at 125 g L^{-1} NaCl. Infective phage titers declined rapidly, with no evidence of detectable amplification, and became undetectable before ammonia removal was fully restored, indicating that the duration of the operational response did not directly reflect phage persistence in the liquid phase. The community remained predominantly composed of Proteobacteria, with a high relative abundance

of *Halomonas* and the presence of several genera potentially associated with nitrogen transformations, indicating that the functional decline was not accompanied by widespread elimination of the dominant groups. These findings show that phage cocktails intended for biocontrol may temporarily affect nontarget functions in biologically active systems, even when their propagation hosts do not correspond to the principal microbial groups associated with the function under evaluation. Therefore, as with any bioremediation treatment, its application in saline wastewater treatment systems should be preceded by assessments integrating host range, operating conditions, viral persistence, and the stability of microbial functions.

Author Contributions: Conceptualization, L.R.M., M.P.d.S. and C.C.d.S.; methodology, L.R.M., M.P.d.S. and A.G.d.C.; validation, L.R.M., M.P.d.S. and A.G.d.C.; formal analysis, L.R.M. and J.J.F.S.; investigation, L.R.M., M.P.d.S. and A.G.d.C.; resources, R.S.d.S., S.O.d.P. and C.C.d.S.; data curation, L.R.M. and M.P.d.S.; writing—original draft preparation, L.R.M.; writing—review and editing, L.R.M., M.P.d.S., A.G.d.C., R.S.d.S., S.O.d.P. and C.C.d.S.; visualization, L.R.M. and A.G.d.C.; supervision, R.S.d.S., S.O.d.P. and C.C.d.S.; project administration, C.C.d.S.; funding acquisition, C.C.d.S. All authors have read and agreed to the published version of the manuscript.

Funding: This study was financed by Petróleo Brasileiro S.A. (Petrobras), the scholarships by the Coordenação de Aperfeiçoamento de Pessoal de Nível Superior, Brazil (CAPES), Finance Code 001, and was supported by the Conselho Nacional de Desenvolvimento Científico e Tecnológico (CNPq) and the Fundação de Amparo à Pesquisa do Estado de Minas Gerais (FAPEMIG).

Data Availability Statement: The raw 16S rRNA gene sequencing data generated in this study were deposited in the NCBI Sequence Read Archive (SRA) under BioProject accession number PRJNA1533409 and will be publicly available upon publication. Additional data supporting the findings of this study are available within the article.

Acknowledgments: The authors acknowledge the Fundação de Amparo à Pesquisa do Estado de Minas Gerais (FAPEMIG), the Coordenação de Aperfeiçoamento de Pessoal de Nível Superior (CAPES), Finance Code 001, and the Conselho Nacional de Desenvolvimento Científico e Tecnológico (CNPq) for their financial and institutional support. The authors also thank Petróleo Brasileiro S.A. (Petrobras) for providing the produced water and for its technical support.

Conflicts of Interest: Authors Maíra Paula de Sousa and Rodrigo Suhett de Souza were employed by Petrobras. The remaining authors declare that the research was conducted in the absence of any commercial or financial relationships that could be construed as a potential conflict of interest.

Abbreviations

The following abbreviations are used in this manuscript:

Abbreviation	Definition
ASV	Amplicon sequence variant
DNA	Deoxyribonucleic acid
NCBI	National Center for Biotechnology Information
ND	Not detected
PCoA	Principal coordinates analysis
PCR	Polymerase chain reaction
PERMANOVA	Permutational multivariate analysis of variance
PFU	Plaque-forming unit
rRNA	Ribosomal ribonucleic acid
SRA	Sequence Read Archive

Appendix A

Table A1. Pairwise comparisons of ammonia removal between control and phage-cocktail-treated microcosms at each sampling time. Two-sided independent-samples *t*-tests were performed separately for each salinity, with Holm-adjusted $p \leq 0.05$ indicating statistical significance. Day indicates the time after phage cocktail application.

Salinity (g L^{-1} NaCl)	Day	Comparison	Unadjusted *p*-Value	Holm-Adjusted *p*-Value	Significant
55	0	Control vs. Phage cocktail	0.295882	0.762937	No
55	1	Control vs. Phage cocktail	0.002868	0.020076	Yes
55	2	Control vs. Phage cocktail	0.000268	0.002416	Yes
55	6	Control vs. Phage cocktail	0.003365	0.020191	Yes
55	8	Control vs. Phage cocktail	0.001839	0.014716	Yes
55	13	Control vs. Phage cocktail	0.062990	0.314950	No
55	16	Control vs. Phage cocktail	0.091234	0.364936	No
55	20	Control vs. Phage cocktail	0.254312	0.762937	No
55	55	Control vs. Phage cocktail	0.298243	0.762937	No
125	0	Control vs. Phage cocktail	0.279146	0.558292	No
125	1	Control vs. Phage cocktail	0.008333	0.041664	Yes
125	2	Control vs. Phage cocktail	0.005571	0.033427	Yes
125	6	Control vs. Phage cocktail	0.002806	0.019644	Yes
125	8	Control vs. Phage cocktail	0.001955	0.015642	Yes
125	13	Control vs. Phage cocktail	0.000797	0.007173	Yes
125	16	Control vs. Phage cocktail	0.014117	0.050924	No
125	20	Control vs. Phage cocktail	0.012731	0.050924	No
125	55	Control vs. Phage cocktail	0.320456	0.558292	No

References

1. Fakhru'l-Razi, A.; Pendashteh, A.; Abdullah, L.C.; Biak, D.R.A.; Madaeni, S.S.; Abidin, Z.Z. Review of technologies for oil and gas produced water treatment. *J. Hazard. Mater.* **2009**, *170*, 530–551. [CrossRef] [PubMed]
2. Neff, J.M.; Lee, K.; DeBlois, E.M. Produced water: Overview of composition. fates. and effects. In *Produced Water: Environmental Risks and Advances in Mitigation Technologies*; Lee, K., Neff, J., Eds.; Springer: New York, NY, USA, 2011; pp. 3–54. [CrossRef]
3. Igunnu, E.T.; Chen, G.Z. Produced water treatment technologies. *Int. J. Low-Carbon Technol.* **2014**, *9*, 157–177. [CrossRef]
4. Jiménez, S.; Micó, M.M.; Arnaldos, M.; Medina, F.; Contreras, S. State of the art of produced water treatment. *Chemosphere* **2018**, *192*, 186–208. [CrossRef] [PubMed]
5. Al-Ghouti, M.A.; Al-Kaabi, M.A.; Ashfaq, M.Y.; Da'na, D.A. Produced water characteristics. treatment and reuse: A review. *J. Water Process Eng.* **2019**, *28*, 222–239. [CrossRef]
6. Quartaroli, L.; Silva, L.C.F.; Silva, C.M.; Lima, H.S.; de Paula, S.O.; Dias, R.S.; de Oliveira, V.M.; Silva, C.C. Ammonium removal from high-salinity oilfield-produced water: Assessing the microbial community dynamics at increasing salt concentrations. *Appl. Microbiol. Biotechnol.* **2017**, *101*, 859–870. [CrossRef] [PubMed]
7. Rittmann, B.E.; McCarty, P.L. *Environmental Biotechnology: Principles and Applications*, 2nd ed.; McGraw Hill: New York, NY, USA, 2020.
8. Fu, W.; Song, G.; Wang, Y.; Wang, Q.; Duan, P.; Liu, C.; Zhang, X.; Rao, Z. Advances in research into and applications of heterotrophic nitrifying and aerobic denitrifying microorganisms. *Front. Environ. Sci.* **2022**, *10*, 887093. [CrossRef]
9. Silva, L.C.F.; Lima, H.S.; Mendes, T.A.O.; Sartoratto, A.; Sousa, M.P.; de Souza, R.S.; de Paula, S.O.; de Oliveira, V.M.; Silva, C.C. Physicochemical characterization of *Pseudomonas stutzeri* UFV5 and analysis of its transcriptome under heterotrophic nitrification/aerobic denitrification pathway induction condition. *Sci. Rep.* **2020**, *10*, 2215. [CrossRef] [PubMed]
10. Medina, L.R.; Silva, L.C.F.; Lima, H.S.; Vidigal, P.M.P.; Castro, A.G.; Sousa, M.P.; de Souza, R.S.; de Paula, S.O.; da Silva, C.C. Genomic insights into heterotrophic nitrifying-aerobic denitrifying bacteria from petroleum terminal effluents. *Heliyon* **2024**, *10*, e39436. [CrossRef] [PubMed]
11. Xia, L.; Li, X.; Fan, W.; Wang, J. Heterotrophic nitrification and aerobic denitrification by a novel *Acinetobacter* sp. ND7 isolated from municipal activated sludge. *Bioresour. Technol.* **2020**, *301*, 122749. [CrossRef] [PubMed]
12. Yao, S.; Ni, J.; Ma, T.; Li, C. Heterotrophic nitrification and aerobic denitrification at low temperature by a newly isolated bacterium. *Acinetobacter* sp. HA2. *Bioresour. Technol.* **2013**, *139*, 80–86. [CrossRef] [PubMed]

13. Zhou, X.; Wang, Y.; Tan, X.; Sheng, Y.; Li, Y.; Zhang, Q.; Xu, J.; Shi, Z. Genomics and nitrogen metabolic characteristics of a novel heterotrophic nitrifying-aerobic denitrifying bacterium *Acinetobacter oleivorans* AHP123. *Bioresour. Technol.* **2023**, *375*, 128822. [CrossRef] [PubMed]
14. Moussa, M.S.; Sumanasekera, D.U.; Ibrahim, S.H.; Lubberding, H.J.; Hooijmans, C.M.; Gijzen, H.J.; van Loosdrecht, M.C.M. Long-term effects of salt on activity. population structure and floc characteristics in enriched bacterial cultures of nitrifiers. *Water Res.* **2006**, *40*, 1377–1388. [CrossRef] [PubMed]
15. Cortés-Lorenzo, C.; Rodríguez-Díaz, M.; Sipkema, D.; Juárez-Jiménez, B.; Rodelas, B.; Smidt, H.; González-López, J. Effect of salinity on nitrification efficiency and structure of ammonia-oxidizing bacterial communities in a submerged fixed-bed bioreactor. *Chem. Eng. J.* **2015**, *266*, 233–240. [CrossRef]
16. Clokie, M.R.J.; Millard, A.D.; Letarov, A.V.; Heaphy, S. Phages in nature. *Bacteriophage* **2011**, *1*, 31–45. [CrossRef] [PubMed]
17. Dion, M.B.; Oechslin, F.; Moineau, S. Phage diversity, genomics and phylogeny. *Nat. Rev. Microbiol.* **2020**, *18*, 125–138. [CrossRef] [PubMed]
18. Kortright, K.E.; Chan, B.K.; Koff, J.L.; Turner, P.E. Phage therapy: A renewed approach to combat antibiotic-resistant bacteria. *Cell Host Microbe* **2019**, *25*, 219–232. [CrossRef] [PubMed]
19. Abedon, S.T.; Kuhl, S.J.; Blasdel, B.G.; Kutter, E.M. Phage treatment of human infections. *Bacteriophage* **2011**, *1*, 66–85. [CrossRef] [PubMed]
20. Shapiro, O.H.; Kushmaro, A. Bacteriophage ecology in environmental biotechnology processes. *Curr. Opin. Biotechnol.* **2011**, *22*, 449–455. [CrossRef] [PubMed]
21. Enning, D.; Garrelfs, J. Corrosion of iron by sulfate-reducing bacteria: New views of an old problem. *Appl. Environ. Microbiol.* **2014**, *80*, 1226–1236. [CrossRef] [PubMed]
22. Gieg, L.M.; Jack, T.R.; Foght, J.M. Biological souring and mitigation in oil reservoirs. *Appl. Microbiol. Biotechnol.* **2011**, *92*, 263–282. [CrossRef] [PubMed]
23. Lu, T.K.; Collins, J.J. Dispersing biofilms with engineered enzymatic bacteriophage. *Proc. Natl. Acad. Sci. USA* **2007**, *104*, 11197–11202. [CrossRef] [PubMed]
24. Donlan, R.M. Preventing biofilms of clinically relevant organisms using bacteriophage. *Trends Microbiol.* **2009**, *17*, 66–72. [CrossRef] [PubMed]
25. Harper, D.R.; Parracho, H.M.R.T.; Walker, J.; Sharp, R.; Hughes, G.; Werthén, M.; Lehman, S.; Morales, S. Bacteriophages and biofilms. *Antibiotics* **2014**, *3*, 270–284. [CrossRef]
26. Weinbauer, M.G. Ecology of prokaryotic viruses. *FEMS Microbiol. Rev.* **2004**, *28*, 127–181. [CrossRef] [PubMed]
27. Suttle, C.A. Marine viruses: Major players in the global ecosystem. *Nat. Rev. Microbiol.* **2007**, *5*, 801–812. [CrossRef] [PubMed]
28. Otawa, K.; Lee, S.H.; Yamazoe, A.; Onuki, M.; Satoh, H.; Mino, T. Abundance, diversity, and dynamics of viruses on microorganisms in activated sludge processes. *Microb. Ecol.* **2007**, *53*, 143–152. [CrossRef] [PubMed]
29. Parsley, L.C.; Consuegra, E.J.; Thomas, S.J.; Bhavsar, J.; Land, A.M.; Bhuiyan, N.N.; Mazher, M.A.; Waters, R.J.; Wommack, K.E.; Harper, W.F., Jr.; et al. Census of the viral metagenome within an activated sludge microbial assemblage. *Appl. Environ. Microbiol.* **2010**, *76*, 2673–2677. [CrossRef] [PubMed]
30. Chen, Y.; Wang, Y.; Paez-Espino, D.; Polz, M.F.; Zhang, T. Prokaryotic viruses impact functional microorganisms in nutrient removal and carbon cycle in wastewater treatment plants. *Nat. Commun.* **2021**, *12*, 5398. [CrossRef] [PubMed]
31. Vieira, M.S.; Dias, R.S.; Lima, H.S.; de Sousa, M.P.; da Silva, C.C.; de Paula, S.O. Influence of a Bacteriophage Cocktail as a Biocontrol Strategy on Sulfate-Reducing Bacteria in a Pilot-Scale System. *Bioengineering* **2026**, *13*, 1166. [CrossRef] [PubMed]
32. Chaney, A.L.; Marbach, E.P. Modified reagents for determination of urea and ammonia. *Clin. Chem.* **1962**, *8*, 130–132. [CrossRef]
33. Zhang, Q.L.; Liu, Y.; Ai, G.M.; Miao, L.L.; Zheng, H.Y.; Liu, Z.P. The characteristics of a novel heterotrophic nitrification–aerobic denitrification bacterium, *Bacillus methylotrophicus* strain L7. *Bioresour. Technol.* **2012**, *108*, 35–44. [CrossRef] [PubMed]
34. Barr, J.J.; Slater, F.R.; Fukushima, T.; Bond, P.L. Evidence for bacteriophage activity causing community and performance changes in a phosphorus-removal activated sludge. *FEMS Microbiol. Ecol.* **2010**, *74*, 631–642. [CrossRef] [PubMed]
35. Shapiro, O.H.; Kushmaro, A.; Brenner, A. Bacteriophage predation regulates microbial abundance and diversity in a full-scale bioreactor treating industrial wastewater. *ISME J.* **2010**, *4*, 327–336. [CrossRef] [PubMed]
36. Liao, Y.; Zhang, J.; Wang, M.; Wu, Y.; Zhang, J.; Wang, S.; Pan, Y.; Cao, G. Nitrogen removal from wastewater for heterotrophic nitrification-aerobic denitrification bacterium with the combination of bacteriophage DEY7 and Fe nanoparticles. *Biochem. Eng. J.* **2023**, *191*, 108805. [CrossRef]
37. Khan, M.A.; Satoh, H.; Katayama, H.; Kurisu, F.; Mino, T. Bacteriophages isolated from activated sludge processes and their polyvalency. *Water Res.* **2002**, *36*, 3364–3370. [CrossRef] [PubMed]
38. Liu, J.; Chu, G.; Wang, Q.; Zhang, Z.; Lu, S.; She, Z.; Zhao, Y.; Jin, C.; Guo, L.; Ji, J.; et al. Metagenomic analysis and nitrogen removal performance evaluation of activated sludge from a sequencing batch reactor under different salinities. *J. Environ. Manag.* **2022**, *323*, 116213. [CrossRef] [PubMed]

39. Campos, J.L.; Mosquera-Corral, A.; Sánchez, M.; Méndez, R.; Lema, J.M. Nitrification in saline wastewater with high ammonia concentration in an activated sludge unit. *Water Res.* **2002**, *36*, 2555–2560. [CrossRef] [PubMed]
40. Bassin, J.P.; Kleerebezem, R.; Muyzer, G.; Rosado, A.S.; van Loosdrecht, M.C.M.; Dezotti, M. Effect of different salt adaptation strategies on the microbial diversity, activity, and settling of nitrifying sludge in sequencing batch reactors. *Appl. Microbiol. Biotechnol.* **2012**, *93*, 1281–1294. [CrossRef] [PubMed]
41. Allison, S.D.; Martiny, J.B.H. Resistance, resilience, and redundancy in microbial communities. *Proc. Natl. Acad. Sci. USA* **2008**, *105*, 11512–11519. [CrossRef] [PubMed]
42. Vuono, D.C.; Benecke, J.; Henkel, J.; Navidi, W.C.; Cath, T.Y.; Munakata-Marr, J.; Spear, J.R.; Drewes, J.E. Disturbance and temporal partitioning of the activated sludge metacommunity. *ISME J.* **2015**, *9*, 425–435. [CrossRef] [PubMed]
43. Santillan, E.; Phua, W.X.; Constancias, F.; Wuertz, S. Sustained organic loading disturbance favors nitrite accumulation in bioreactors with variable resistance, recovery and resilience of nitrification and nitrifiers. *Sci. Rep.* **2020**, *10*, 21388. [CrossRef] [PubMed]
44. Ewert, D.L.; Paynter, M.J.B. Enumeration of bacteriophages and host bacteria in sewage and the activated-sludge treatment process. *Appl. Environ. Microbiol.* **1980**, *39*, 576–583. [CrossRef] [PubMed]
45. Runa, V.; Wenk, J.; Bengtsson, S.; Jones, B.V.; Lanham, A.B. Bacteriophages in biological wastewater treatment systems: Occurrence, characterization. and function. *Front. Microbiol.* **2021**, *12*, 730071. [CrossRef] [PubMed]
46. Stocks, S.M. Mechanism and use of the commercially available viability stain. *BacLight Cytom. Part A* **2004**, *61A*, 189–195. [CrossRef] [PubMed]
47. Berney, M.; Hammes, F.; Bosshard, F.; Weilenmann, H.U.; Egli, T. Assessment and interpretation of bacterial viability by using the LIVE/DEAD BacLight Kit in combination with flow cytometry. *Appl. Environ. Microbiol.* **2007**, *73*, 3283–3290. [CrossRef] [PubMed]
48. Stiefel, P.; Schmidt-Emrich, S.; Maniura-Weber, K.; Ren, Q. Critical aspects of using bacterial cell viability assays with the fluorophores SYTO9 and propidium iodide. *BMC Microbiol.* **2015**, *15*, 36. [CrossRef] [PubMed]
49. Rosenberg, M.; Azevedo, N.F.; Ivask, A. Propidium iodide staining underestimates viability of adherent bacterial cells. *Sci. Rep.* **2019**, *9*, 6483. [CrossRef] [PubMed]
50. Robertson, J.; McGoverin, C.; Vanholsbeeck, F.; Swift, S. Optimisation of the protocol for the LIVE/DEAD BacLight bacterial viability kit for rapid determination of bacterial load. *Front. Microbiol.* **2019**, *10*, 801. [CrossRef] [PubMed]
51. Osaka, T.; Shirotani, K.; Yoshie, S.; Tsuneda, S. Effects of carbon source on denitrification efficiency and microbial community structure in a saline wastewater treatment process. *Water Res.* **2008**, *42*, 3709–3718. [CrossRef] [PubMed]
52. Ou, D.; Li, H.; Li, W.; Wu, X.; Wang, Y.Q.; Liu, Y.D. Salt-tolerance aerobic granular sludge: Formation and microbial community characteristics. *Bioresour. Technol.* **2018**, *249*, 132–138. [CrossRef] [PubMed]
53. Wang, T.; Li, J.; Zhang, L.H.; Yu, Y.; Zhu, Y.M. Simultaneous heterotrophic nitrification and aerobic denitrification at high concentrations of NaCl and ammonia nitrogen by Halomonas bacteria. *Water Sci. Technol.* **2017**, *76*, 386–395. [CrossRef] [PubMed]
54. Hu, J.; Yan, J.; Wu, L.; Bao, Y.; Yu, D.; Li, J. Simultaneous nitrification and denitrification of hypersaline wastewater by a robust bacterium Halomonas salifodinae from repeated-batch acclimation. *Bioresour. Technol.* **2021**, *341*, 125818. [CrossRef] [PubMed]
55. Hu, J.; Yan, J.; Wu, L.; Bao, Y.; Yu, D.; Li, J. Insight into halotolerance of a robust heterotrophic nitrifying and aerobic denitrifying bacterium Halomonas salifodinae. *Bioresour. Technol.* **2022**, *351*, 126925. [CrossRef] [PubMed]
56. Louca, S.; Polz, M.F.; Mazel, F.; Albright, M.B.N.; Huber, J.A.; O'Connor, M.I.; Ackermann, M.; Hahn, A.S.; Srivastava, D.S.; Crowe, S.A.; et al. Function and functional redundancy in microbial systems. *Nat. Ecol. Evol.* **2018**, *2*, 936–943. [CrossRef] [PubMed]
57. Cui, Y.W.; Zhang, H.Y.; Ding, J.R.; Peng, Y.Z. The effects of salinity on nitrification using halophilic nitrifiers in a sequencing batch reactor treating hypersaline wastewater. *Sci. Rep.* **2016**, *6*, 24825. [CrossRef] [PubMed]
58. Louca, S.; Parfrey, L.W.; Doebeli, M. Decoupling function and taxonomy in the global ocean microbiome. *Science* **2016**, *353*, 1272–1277. [CrossRef] [PubMed]

Disclaimer/Publisher's Note: The statements, opinions and data contained in all publications are solely those of the individual author(s) and contributor(s) and not of MDPI and/or the editor(s). MDPI and/or the editor(s) disclaim responsibility for any injury to people or property resulting from any ideas, methods, instructions or products referred to in the content.